AGU PUBLICATIONS

Geophysical Research Letters

RESEARCH LETTER
10.1002/2015GL063937

Key Points:
- Approximately 20% of tropical lower stratospheric air originates at the Asian boundary layer
- Asian air reaches the tropical stratosphere within days of leaving the surface
- Origin tracers are rigorous and practical tools for assessing model transport

Correspondence to:
C. Orbe,
clara.orbe@nasa.gov

Citation:
Orbe, C., D. W. Waugh, and P. A. Newman (2015), Air-mass origin in the tropical lower stratosphere: The influence of Asian boundary layer air, *Geophys. Res. Lett.*, *42*, doi:10.1002/2015GL063937.

Received 20 MAR 2015
Accepted 29 APR 2015
Accepted article online 4 MAY 2015

Air-mass origin in the tropical lower stratosphere: The influence of Asian boundary layer air

Clara Orbe[1], Darryn W. Waugh[2], and Paul A. Newman[1]

[1]Laboratory for Atmospheric Chemistry and Dynamics, NASA Goddard Space Flight Center, Greenbelt, Maryland, USA, [2]Department of Earth and Planetary Sciences, Johns Hopkins University, Baltimore, Maryland, USA

Abstract A climatology of air-mass origin in the tropical lower stratosphere is presented for the Goddard Earth Observing System Chemistry Climate Model. During late boreal summer and fall, air-mass fractions reveal that as much as 20% of the air in the tropical lower stratosphere last contacted the planetary boundary layer (PBL) over Asia; by comparison, the air-mass fractions corresponding to last PBL contact over North America and over Europe are negligible. Asian air reaches the extratropical tropopause within a few days of leaving the boundary layer and is quasi-horizontally transported into the tropical lower stratosphere, where it persists until January. The rapid injection of Asian air into the lower stratosphere—and its persistence in the deep tropics through late (boreal) winter—is important as industrial emissions over East Asia continue to increase. Hence, the Asian monsoon may play an increasingly important role in shaping stratospheric composition.

1. Introduction

Observations and models provide strong evidence that trace species and aerosols that are emitted at the planetary boundary layer (PBL) are transported into the stratosphere, where they impact ozone and climate. For example, the troposphere-to-stratosphere transport of water vapor, a potent greenhouse gas, can perturb the radiative balance in the atmosphere by cooling the stratosphere and warming the troposphere [e.g., *Forster and Shine*, 1999; *Shindell*, 2001; *Forster and Shine*, 2002]. Studies have also shown that short-lived halogens released at the PBL have been nearly half as effective as long-lived halocarbons at depleting ozone in recent decades, by increasing the stratospheric burdens of reactive bromine and chlorine [e.g., *Sinnhuber et al.*, 2002; *Liang et al.*, 2010; *Hossaini et al.*, 2015].

There is strong evidence from models and observations that a wide range of pathways connect the PBL to the lower stratosphere. In addition to the large-scale troposphere-to-stratosphere transport that occurs in the deep tropics throughout the year [*Fueglistaler et al.*, 2004], the Asian monsoon provides an effective transport pathway that connects the extratropical boundary layer to the lower stratosphere [*Randel et al.*, 2010]. Signatures of the monsoon anticyclone have been observed in the distributions of methane and nitrogen oxides [*Park et al.*, 2004], water vapor [*Rosenlof et al.*, 1997; *Ploeger et al.*, 2013; *Vogel et al.*, 2014], and several hydrocarbons, including carbon monoxide, ethane, and acetylene [*Park et al.*, 2013]. More recently, observations have also revealed enhanced aerosol backscatter over Asia during boreal summer as sulfur dioxide, of both volcanic and industrial origin, is organized within the large-scale upper level divergent circulation associated with the monsoon [*Vernier et al.*, 2011a; *Bourassa et al.*, 2012; *Thomason and Vernier*, 2013; *Neely et al.*, 2013]. This is important given the contributions that tropospheric sources of sulfur dioxide make to the variability—and, possibly, long-term trends—of the stratospheric aerosol layer, an important component in maintaining the radiative balance in the atmosphere [*Hofmann et al.*, 2009; *Solomon et al.*, 2011].

As comprehensive climate models are used to assess future changes in stratospheric ozone and aerosol, the fidelity of their projections will hinge partly on how well they capture the wide range of transport pathways that connect the tropical and extratropical PBL to the lower stratosphere. Hence, meaningful diagnostics for assessing model transport must account for the fact that the air in the lower stratosphere reflects the mixture of air masses that originated at different regions over the PBL. While the mean age [*Hall and Plumb*, 1994] has been used extensively to compare stratospheric transport among comprehensive climate models [*CCMVal*, 2010], there is no suitable tracer-independent diagnostic for assessing transport out of the planetary boundary layer and into the lower stratosphere. (By "tracer-independent" we mean independent of species' chemistry and emissions patterns).

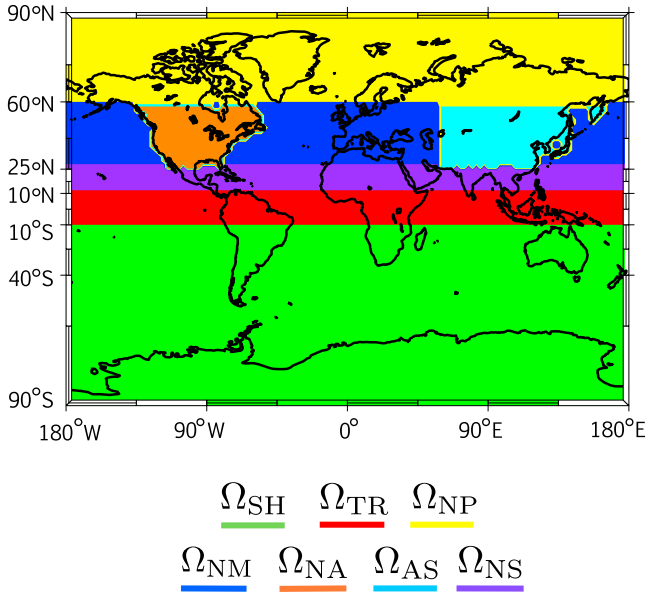

Figure 1. The Ω_i regions where the air-mass fractions last contacted the PBL. Zonal strips of fixed width span latitudes south of 10°S (Ω_{SH}) and tropical latitudes between 10°S and 10°N (Ω_{TR}). The PBL north of 10°N (Ω_{NH}) is partitioned into Ω_i regions overlying the subtropics ($\Omega_{NS} \in [10°N, 25°N]$), midlatitudes ($\Omega_{NM} \in [25°N, 60°N]$), and the north polar region ($\Omega_{NP} \in [60°N, 90°N]$). The orange and cyan patches overlay North America (Ω_{NA}) and Asia (Ω_{AS}), respectively.

One tracer-independent diagnostic that is both conceptually simple and straightforward to calculate is the origin of air over the PBL. The origin of air over the PBL represents a fundamental property of the transport climate that is especially relevant to short-lived species emitted in the troposphere that do not survive transit into and out of the stratosphere. Air-mass origin can be naturally quantified using synthetic tracers that capture the atmosphere's advective-diffusive transport operator, independent of any particular trace species. Specifically, the air-mass fraction $f(\mathbf{r}, t|\Omega_i)$ is defined to be the mass fraction of air at a location $\mathbf{r}$ and time t that had last contact with the PBL in region Ω_i, and not elsewhere. In practice, air-mass origin can be calculated as simple equilibrated tracer mixing ratios with boundary conditions specified so that they reveal where, and with what dilution, the air from various sources can be found.

Water-mass fractions, the oceanography equivalent of air-mass fractions, have long been used to study transport in the oceans [*Tomczak*, 1981; *Haine and Hall*, 2002; *Holzer et al.*, 2010] and, more recently, have been applied to atmospheric transport [*Orbe et al.*, 2013, 2015]. Here we present the first seasonally varying climatology of air-mass origin in the tropical lower stratosphere for the modeled climate of the Goddard Earth Observing System Chemistry Climate Model (GEOSCCM) forced with present-day greenhouse gases and ozone depleting substances.

2. Methods

Air-mass origin is defined with respect to the planetary boundary layer, denoted by Ω, which we divide into three zonally symmetric origin regions, Ω_i, that span latitudes south of 10°S (Ω_{SH}), latitudes between 10°S and 10°N (Ω_{TR}), and latitudes poleward of 10°N (Ω_{NH}) (Figure 1). Within Ω_{NH} we also define zonal strips spanning the NH subtropics ($\Omega_{NS} \in [10°N, 25°N]$), midlatitudes ($\Omega_{NM} \in [25°N, 60°N]$), and the north polar region ($\Omega_{NP} \in [60°N, 90°N]$). In addition, the Ω_{NM} origin region is partitioned still further into patches consisting of North America (Ω_{NA}) and Asia (Ω_{AS}), in order to assess the relative presence of North American and Asian boundary layer air in the lower stratosphere, as this remains an open question [*Gettelman et al.*, 2004; *Randel et al.*, 2010, 2012]. For each of the Ω_i origin regions, $f(\mathbf{r}, t|\Omega_i)$ is computed as the solution to the passive tracer advection/diffusion equation in the interior of the atmosphere (that is, outside of Ω) and is held to be unity in Ω_i and equal to zero in the rest of Ω [*Orbe et al.*, 2013].

Calculations are performed using the same integration of the Goddard Earth Observing System Chemistry Climate Model Version 2 (GEOSCCM) presented in *Orbe et al.* [2015], in which the GEOS-5 GCM [*Suarez et al.*, 2008] is coupled with a comprehensive stratospheric chemistry package [*Douglass et al.*, 1996]. The model has a

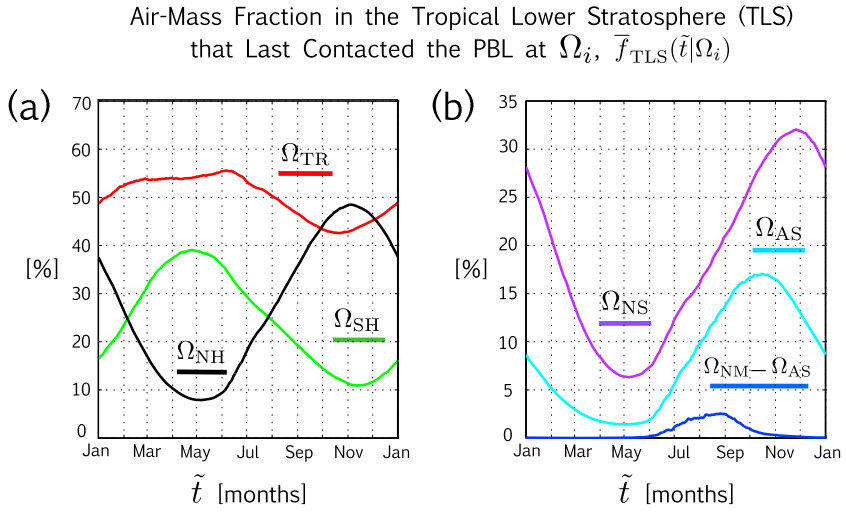

Figure 2. (a) Seasonal cycle of the Ω_i air-mass fraction in the tropical lower stratosphere (TLS) (i.e., the average over 20°S–20°N and 70–100 mb), where $\tilde{t}$ denotes the month of year when air is in transit in the TLS. Origin at the PBL is shown with respect to Ω_{SH} (green), Ω_{TR} (red), and Ω_{NH} (black). (Note that, because Ω_{SH}, Ω_{TR}, and Ω_{NH} span the entire PBL, Ω, the sum of their corresponding air-mass fractions is 100% for all $\tilde{t}$.) (b) Seasonal cycle of the Ω_{NH} air-mass fraction, further partitioned between origin over Ω_{NS} (purple) and Ω_{AS} (cyan). All remaining air of midlatitude origin, $\Omega_{NM}-\Omega_{AS}$, is shown in the blue line. Note that the contribution from Ω_{NP} is not shown, as it is negligible.

horizontal resolution of 2° latitude by 2.5° longitude with 72 vertical levels extending from the surface to 0.01 hPa and is forced with annually repeating 2000–2019 time-averaged greenhouse gases and ozone-depleting substances under the A1B and A1 scenarios, respectively [*McCarthy*, 2001; *WMO*, 2007]. Note that in the model, the linear advective diffusion transport operator includes parameterized subgrid-scale processes such as convection, which is treated in GEOSCCM using the Relaxed Arakawa-Schubert convective scheme [*Moorthi and Suarez*, 1992], a modified version of the Arakawa-Schubert scheme [*Arakawa and Schubert*, 1974]. The reader is referred to *Orbe et al.* [2015] for more details about the model configuration.

Spin-up to a statistically stationary state for the dynamical variables (not the tracers) takes 10 years, after which we introduce our diagnostic tracers that are passively advected using a flux-form semi-Lagrangian transport scheme [*Lin and Rood*, 1996] for an additional 20 years, after which the air-mass fractions have equilibrated. The model's transport in the stratosphere has been assessed extensively in previous studies [e.g., *Pawson et al.*, 2008; *Douglass et al.*, 2008; *CCMVal*, 2010], which show that GEOSCCM performs well in terms of its stratospheric mean age and representation of ascent within the tropics. The fidelity of the model's treatment of shorter-lived species is also examined in *Liang et al.* [2010], who show that the upper tropospheric and lower stratospheric distributions of bromoform and dibromomethane produced in GEOSCCM compare well with measurements obtained from aircraft.

At steady state, after which the air-mass fractions have equilibrated (i.e., $f(\mathbf{r}, t|\Omega_i) \rightarrow \overline{f}(\mathbf{r}|\Omega_i)$), the boundary conditions ensure that the sum of $f(\mathbf{r}|\Omega_i)$ over all Ω_i overlying the PBL (here the union of Ω_{SH}, Ω_{TR}, and Ω_{NH}), is equal to unity throughout the entire atmosphere [*Orbe et al.*, 2013]. (Throughout, the overbar denotes the average of the air-mass fraction over the last 10 years of the integration). For convenience, the air-mass fraction corresponding to the region Ω_i will be referred throughout as "Ω_i-air." For example, Ω_{SH}-air (also "southern hemisphere (SH) air" or "air of southern hemisphere origin") will refer to the air-mass fraction that last encountered the PBL south of 10°S.

3. Results

3.1. Air-Mass Origin in the Tropical Lower Stratosphere: Last Contact Over Ω_{SH}, Ω_{TR}, and Ω_{NH}

To first order, roughly half of the air in the tropical lower stratosphere (TLS)—herein defined as the region spanning 20°S–20°N and 70–100 mb—last contacted the PBL in the deep tropics (10°S–10°N) (Figure 2a). The seasonal cycle of the air-mass fractions, $\overline{f}_{\rm TLS}(\tilde{t}|\Omega_i)$, where $\tilde{t}$ is the month of year when air is in transit in the tropical lower stratosphere, reveals that during boreal spring and early summer, most of the remaining air is of southern (Ω_{SH}) origin; conversely, the remaining air is primarily of northern (Ω_{NH}) origin throughout boreal fall

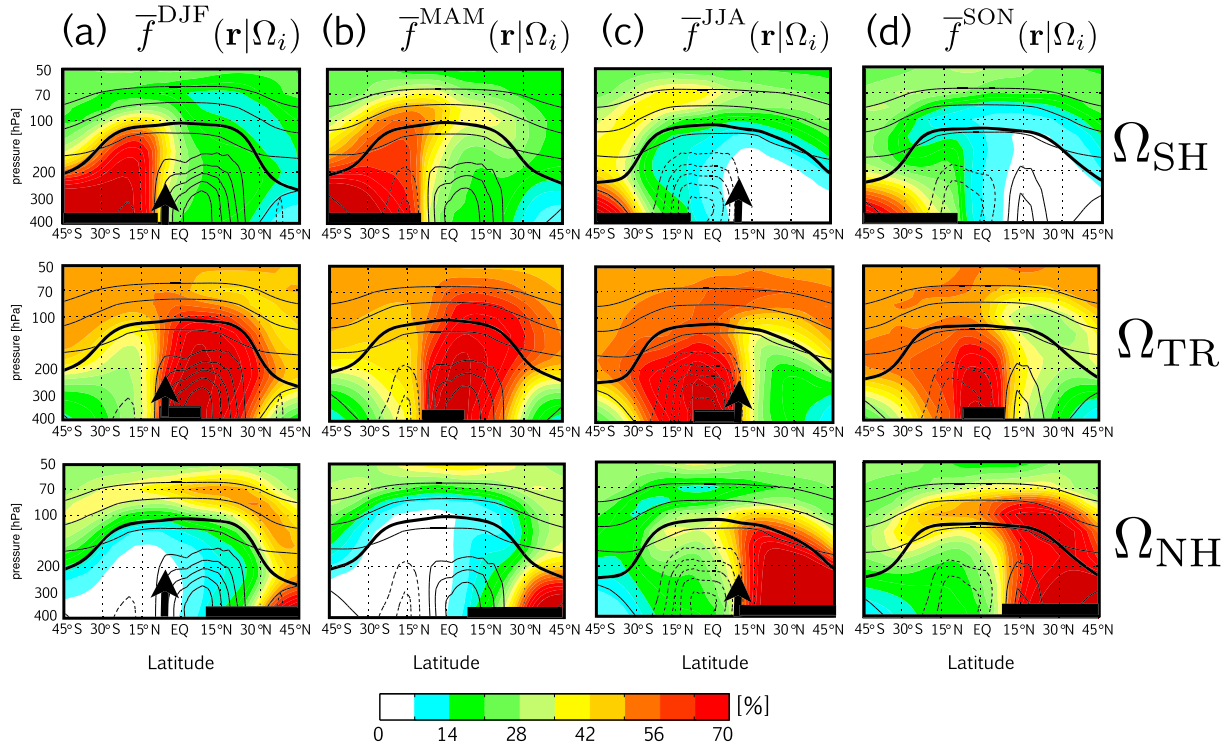

Figure 3. (a) The boreal winter (December-January-February, DJF) climatological air-mass fraction $\overline{f}^{\mathrm{DJF}}(\mathbf{r}|\Omega_i)$, corresponding to air that last contacted the PBL over Ω_{SH} (top), Ω_{TR} (middle), and Ω_{NH} (bottom). The zonal mean wintertime thermal tropopause is indicated by the thick black line; zonally averaged boreal wintertime mean isentropes are overlaid in the thin black lines (contour interval: 20 K for isentropes between 280 and 360 K; 40 K interval for isentropes greater than 360 K). The seasonally averaged stream function (contour interval: 60×10^9 kg/s) has also been overlaid on all panels, in order to provide a sense for the zonally averaged tropospheric circulation in the tropics and subtropics. (b–d) Same as Figure 3a but for March-April-May (MAM), June-July-August (JJA), and September-October-November (SON), respectively. Throughout, black boxes designate the corresponding Ω_i region.

and early winter. (Note that, because Ω_{SH}, Ω_{TR}, and Ω_{NH} together span the PBL, the sum of their corresponding air-mass fractions is 100%. Physically, this means that the air had to have last contacted the PBL somewhere in its history and provides a useful numerical check for whether equilibrium has been reached).

Large fractions of Ω_{SH}-air in the tropical lower stratosphere during boreal winter reflect the southward shift of the intertropical convergence zone (ITCZ) into the SH subtropics (i.e., south of 10°S) and mean upwelling within the ascending branch of the wintertime Hadley Cell, which draws boundary layer air into the upper troposphere. (Conversely, Ω_{NH}-air encounters mean descent over the NH subtropics (i.e., north of 10°N) and is stripped of its origin label at neighboring latitudes). During boreal summer, by comparison, when the ITCZ shifts into the NH subtropics, mean upwelling transports Ω_{NH}-air into the upper tropical troposphere. The correspondence between the Hadley Cell and the air-mass fractions is transparent in Figure 3, where seasonal mean climatologies of the zonal mean air-mass fractions have been overlaid with the mean stream function, a measure of the tropospheric mean mass transport circulation.

The fact that $\overline{f}_{\mathrm{TLS}}(\tilde{t}|\Omega_{\mathrm{NH}})$ and $\overline{f}_{\mathrm{TLS}}(\tilde{t}|\Omega_{\mathrm{SH}})$ maximize during May and September—nearly 2 months lagged relative to the tropical upper troposphere (not shown)—reflects the additional time that it takes for air to propagate from the upper troposphere into the tropical lower stratosphere. Large fractions of Ω_{NH}-air and Ω_{SH}-air persist in the tropical lower stratosphere several months after crossing the tropopause, as there is little chance of boundary layer air being relabeled at the PBL. Correspondingly, nearly 40% of the air in the TLS region is of Northern Hemisphere origin in January (Figure 2a).

3.2. Origin of Northern Hemisphere Air in the Lower Stratosphere

Further partitioning $\overline{f}_{\mathrm{TLS}}(\tilde{t}|\Omega_{\mathrm{NH}})$ into air that originated over the NH subtropics and midlatitudes, we find that between 55–75% and 25–45% of Ω_{NH}-air in the tropical lower stratosphere last contacted the PBL over Ω_{NS} and Ω_{AS}, respectively (Figure 2b). By comparison, no more than ~5% of Northern Hemisphere air in the TLS region originated over any other region at NH midlatitudes (i.e., neither North America nor Europe,

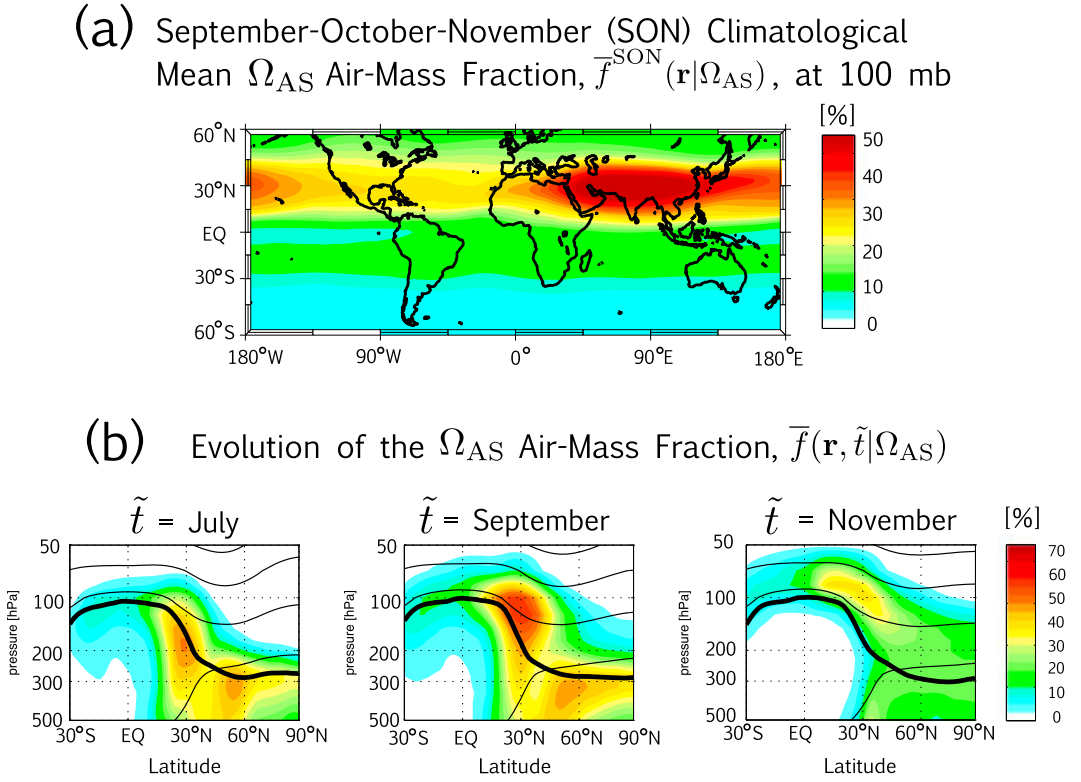

Figure 4. (a) The SON climatological air-mass fraction that last contacted the PBL over Asia, $\overline{f}^{SON}(\mathbf{r}|\Omega_{AS})$, evaluated at 100 mb. (b) Climatological monthly mean air-mass fractions $\overline{f}(\mathbf{r}, \tilde{t}|\Omega_{AS})$ for $\tilde{t}$ = July, September, and November. The zonally averaged monthly mean thermal tropopause is indicated by the thick black line; zonally averaged monthly mean isentropes are overlaid in the thin black lines (contour interval: 20 K). Note that only latitudes north of 30°S are shown.

both regions of strong industrial emissions), while the contribution from air originating poleward of 60°N is negligible.

Interestingly, there is significantly less Asian boundary layer air in the tropical upper troposphere than in the tropical lower stratosphere (not shown), which suggests that Ω_{AS}-air enters the lower stratosphere first at the extratropical tropopause and is then horizontally entrained into the deep tropics. Correspondingly, the (September-October-November) SON climatological mean distribution of $\overline{f}^{SON}(\mathbf{r}|\Omega_{AS})$ evaluated at 100 mb reveals that Ω_{AS}-air is strongly confined within the monsoon anticyclone over ~30°N (Figure 4a), similar to observed signatures of the monsoon in the distributions of hydrocarbons, methane, and nitrogen oxides, among other species [*Park et al.*, 2004; *Randel et al.*, 2010; *Park et al.*, 2013]. In the middle and upper troposphere Ω_{AS}-air is more or less confined within the anticyclone, which ensures that it is not easily relabeled at the PBL; by comparison, in the lower stratosphere $\overline{f}^{SON}(\mathbf{r}|\Omega_{AS})$ penetrates as far south as 30°S, where ~20% of the air at 100 mb is of Asian origin. Large fractions of Ω_{AS}-air persist long after the monsoon has reached its peak intensity, accounting for nearly 10% of all air in the TLS region in January.

Finally, the monthly evolution of $\overline{f}(\mathbf{r}, \tilde{t}|\Omega_{AS})$ during late summer and early fall provides a gross sense for the pathways that connect the Asian boundary layer to the tropical lower stratosphere (Figure 4b). During July large fractions of Ω_{AS}-air are concentrated at the extratropical tropopause (~30°N). This pattern strongly resembles observed distributions of hydrogen cyanide, a tropospheric pollutant produced in biomass burning that may be interpreted as a tracer of the Asian monsoon, owing to a strong sink from contact with the ocean that ensures its removal in the tropics [*Randel et al.*, 2010]. By September, the Ω_{AS} air-mass fraction extends deep into the tropical lower stratosphere, where it is compensated primarily by reduced fractions of Ω_{TP}-air, consistent with enhanced horizontal mixing in the presence of a weaker tropical/subtropical mixing barrier [*Chen*, 1995]. By comparison, the bulk of Ω_{NS}-air enters the lower stratosphere at the tropical tropopause, in concert with broad large-scale upwelling (not shown).

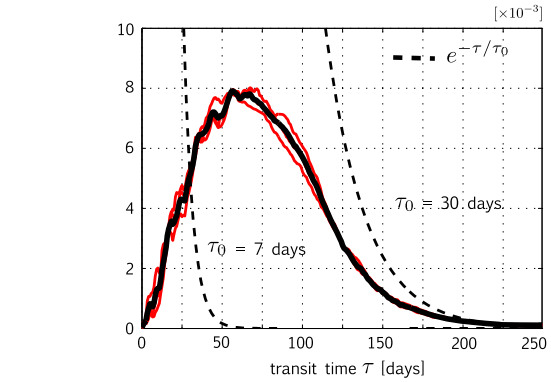

Figure 5. The response to a pulse of conversed tracer released over Ω_{AS} in July, evaluated at 85 mb and averaged over latitudes between 0° and 10°N. The thick black line denotes the ensemble mean response, while red lines denote the individual ensemble members, $\mathcal{G}(\mathbf{r}, t|\Omega_{AS}, \text{July})$, plotted for convenience in terms of the elapsed time or "transit" time $\tau \equiv t - t'$, where t' = July. Dashed lines indicate exponential decay corresponding to *e*-folding times of τ_0 = 7 days and τ_0 = 30 days. The convolution of $e^{-\tau/\tau_0}$ with $\mathcal{G}(\mathbf{r}, \tau|\Omega_{AS}, \text{July})$, integrated over all transit times, yields the fraction of the air released over Ω_{AS} in July that survives transit to the lower stratosphere.

3.3. Asian Boundary Layer Air in the Lower Stratosphere: PBL → Lower Stratosphere Transit Times

The equilibrated air-mass fraction provides a convenient measure of the integrated transport from Ω_{AS} to **r** *independent* of when last PBL contact occurred. However, the concentration of a chemical species (χ) subject to time-varying emissions over Asia and/or chemical decay, will depend on the time it takes for transport to occur from the boundary layer to the tropical lower stratosphere. Because of mixing, however, there is no single PBL → TLS time scale, but rather a distribution of times and the concentration $\chi(\mathbf{r}, t)$ at location **r** and field time t can be expressed in terms of the convolution $\chi(\mathbf{r}, t) = \int_{-\infty}^{t} dt' \mathcal{G}(\mathbf{r}, t|\Omega_{AS}, t') \chi_{\Omega_{AS}}(t') e^{-(t-t')/\tau_0}$, where the mixing ratio of χ at the Asian boundary layer ($\chi_{\Omega_{AS}}$) has been assumed to be spatially uniform and where the exponential term represents chemical decay or physical deposition operating at a time scale τ_0. Here the boundary propagator $\mathcal{G}(\mathbf{r}, t|\Omega_{AS}, t')$ is interpreted as the distribution of transit times $\tau \equiv t - t'$ since the air at $(\mathbf{r}, t)$ was last at Ω_{AS} at time t' [*Holzer and Hall*, 2000].

For the purposes of this study, we focus on a particular instance of the boundary propagator $\mathcal{G}(\mathbf{r}, t|\Omega_{AS}, t')$ at t' = July, henceforth referred to as the Boundary Impulse Response (BIR) [*Haine et al.*, 2008]. This simplification allows us to focus on the response in the tropical lower stratosphere to air that left the PBL in July, when the Asian monsoon is active. (Note that we are not concerned with recovering the full concentration $\chi(\mathbf{r}, t)$ in the lower stratosphere, as this would require knowledge of the boundary propagator evaluated for all t' prior to t). In practice, $\mathcal{G}(\mathbf{r}, t|\Omega_{AS}, \text{July})$ is calculated as the response to a 1 day long pulse of a conserved and passive tracer over Ω_{AS} on 1 July subject to boundary conditions of 1 over Ω_{AS} for the duration of the pulse and 0 over the entire PBL thereafter [*Holzer and Hall*, 2000]. An ensemble of three BIR tracers is computed, one member for each of the first 3 years of the integration following spin-up.

The ensemble-averaged response $\mathcal{G}(\mathbf{r}, \tau|\Omega_{AS}, \text{July})$, evaluated at 85 mb and averaged over latitudes between the equator and 10°N, reveals that a large (~10%) fraction of Asian boundary layer in the NH tropical lower stratosphere arrives within 1 month of leaving the PBL in July (Figure 5: note that $\mathcal{G}$ is expressed, for convenience, in terms of the transit time τ). Overall, the shape of $\mathcal{G}(\mathbf{r}, \tau|\Omega_{AS}, \text{July})$ is consistent with the transit time distributions presented in *Bergman et al.* [2013], calculated using Lagrangian particle trajectories driven by reanalysis winds. An extensive comparison with that study is limited, however, by the fact that *Bergman et al.* [2013] focus on transport into the monsoon anticyclone (i.e., not the ensuing transport into the lower stratosphere). In addition, the spatial pattern of $\mathcal{G}$ evaluated for $\tau < 30$ days (not shown) reveals that Ω_{AS}-air leaves the lower troposphere within a well-defined conduit over the Tibetan Plateau [*Bergman et al.*, 2013], circumvents the tropical upper troposphere, and enters the lower stratosphere at the extratropical tropopause. (Note that the spread between the three ensemble members is relatively small, consistent with the fact that for our modeled climate, where there is no representation of the quasi-biennial oscillation (QBO), seasonal variations trump interannual variability).

The fact that ~10% of Ω_{AS}-air released in July reaches the tropical lower stratosphere in less than 1 month indicates that the monsoon transport pathway may be relevant to a wide range of short-lived trace species, even those with lifetimes as short as 1 week (e.g., the short-lived volatile organic compounds benzene and propane as well as methyl iodide, which are particularly efficient at destroying ozone). More precisely, the convolution

of $\mathcal{G}(\mathbf{r}, \tau|\Omega_{AS}, \text{July})$ with $e^{-\tau/\tau_0}$ (the exponential decay curves shown in Figure 5) is greater than zero, even for the case of rapid decay (i.e., $\tau_0 = 7$ days). This stems from the fact that, while the mean of $\mathcal{G}(\mathbf{r}, \tau|\Omega_{AS}, \text{July})$ is on the order of 1 year, the distribution is skewed to small transit times, so that even short-lived species released at the PBL can survive transit to the lower stratosphere. The lower stratospheric concentrations of species with longer lifetimes (i.e., $\tau_0 = 30$ days) will also reflect the aggregate response to more circuitous transport pathways that respond to large-scale upwelling at the tropical tropopause and in-mixing of midlatitude air into the tropics [*Konopka et al.*, 2009].

4. Conclusions

The interpretation of trace species distributions in the lower stratosphere is complicated by the fact that the air in the lower stratosphere reflects the mixture of air masses that originated over different regions at the PBL. Until now, however, the relative importance of different transport pathways originating at the boundary layer has remained an open question, owing largely to the lack of tracer-independent diagnostics that disentangle transport from species' emissions patterns and chemistry. Air-mass fractions quantify the importance of different boundary layer regions on the composition of the lower stratosphere and for GEOSCCM reveal that

1. During late boreal summer and fall, nearly 20% of the air in the tropical lower stratosphere last contacted the PBL over Asia. By comparison, negligible fractions originate over North America and Europe, where large industrial emissions also prevail.
2. Asian boundary layer air is organized in the upper troposphere within the monsoon anticyclone, enters the stratosphere at the extratropical tropopause (~30°N), and is quasi-horizontally entrained southward into the tropics, where it persists through January. Transport into the tropical lower stratosphere occurs on time scales as short as a few days, rendering this pathway extremely relevant to short-lived trace species.

Given the somewhat limited assessment of how well GEOSCCM represents convective transport from the boundary layer into the tropical upper troposphere, it will be important to explore the sensitivity of our calculations to changes in the convective mass flux and moist physics parameters that inform the model's convection scheme, along the lines of previous studies [*Ott et al.*, 2011]. Model biases in the large-scale circulation—namely, an eastward bias in the location of the Asian monsoon anticyclone compared to MERRA reanalysis—may also affect the quantitative nature of our findings and will be examined in future work [*Molod et al.*, 2012].

Our study has only considered a single integration of GEOSCCM for the current climate and it will also be important to repeat our calculations with other models and for different climate forcings. In particular, few studies have examined how transport will change in response to future warming and the air-mass fractions provide a rigorous way to relate changes in the large-scale circulation to future changes in the distributions of chemical species. As one example, air-mass origin tracers may be used to determine how the ventilation of the tropical and subtropical boundary layer will respond to a weakening and expansion of the Hadley Cell as greenhouse gases increase [e.g., *Lu et al.*, 2007]. An analysis along these lines would have important climate implications, since changes in boundary layer ventilation may affect the transport of short-lived halogens into the upper troposphere and, hence, stratospheric ozone depletion [*Hossaini et al.*, 2015].

Tracers of air-mass origin not only provide a practical framework for comparing model transport—akin to other tracer-independent diagnostics like the mean age [*Hall and Plumb*, 1994]—but can also be studied in the context of a single model. For example, global climate models have recently been used to determine whether volcanic sources of sulfur dioxide or anthropogenic emissions from Asia have contributed to recent trends in stratospheric aerosol [*Vernier et al.*, 2011b; *Neely et al.*, 2013]. The success of this approach, however, depends strongly on how well models represent the underlying transport pathways that connect the Asian boundary layer to the stratosphere, which can be rigorously compared between models using the air-mass origin tracers outlined in this study. The fidelity of model calculations can also be assessed using estimates of the air-mass fractions obtained from observable tracer data, as has been performed for the oceans using simple mixing matrix [e.g., *Tomczak*, 1981] as well as maximum-entropy approaches [*Holzer et al.*, 2010; *Khatiwala et al.*, 2009, 2012].

Air-mass origin tracers may also provide context for interpreting trace gas variability in the tropical lower stratosphere. In a separate analysis, not shown here for the sake of brevity, we find that there are large differences in the amount of Asian boundary layer air in the tropical lower stratosphere between latitudes south and north of the equator. These results may help in the interpretation of the seasonal cycle of lower stratospheric ozone — which is significantly weaker and lagged in the SH tropics compared to the NH tropics [*Stolarski et al.*, 2014] — and, more generally, add to growing evidence that the tropical lower stratosphere is not as well mixed as simple models of stratospheric transport (i.e., the "leaky pipe" model [*Plumb*, 1996; *Neu and Plumb*, 1999]) typically assume. This point will be investigated more closely in future work.

Acknowledgments

This research was supported by an appointment to the NASA Postdoctoral Program at the Goddard Space Flight Center, administered by Oak Ridge Associated Universities through a contract with NASA. The authors also acknowledge support from NSF grant AGS-1403676 (D.W.W.) and NASA grant NNX14AP58G (D.W.W.). The authors are thankful for the discussions with Bill Randel, Laura Pan, and Mijeong Park. All data presented in this paper are available from the corresponding author upon direct request.

The Editor thanks Gang Chen and an anonymous reviewer for their assistance in evaluating this paper.

References

Arakawa, A., and W. H. Schubert (1974), Interaction of a cumulus cloud ensemble with the large-scale environment, Part I, *J. Atmos. Sci.*, *31*(3), 674–701.

Bergman, J. W., F. Fierli, E. J. Jensen, S. Honomichl, and L. L. Pan (2013), Boundary layer sources for the Asian anticyclone: Regional contributions to a vertical conduit, *J. Geophys. Res. Atmos.*, *118*, 2560–2575, doi:10.1002/jgrd.50142.

Bourassa, A. E., A. Robock, W. J. Randel, T. Deshler, L. A. Rieger, N. D. Lloyd, E. T. Llewellyn, and D. A. Degenstein (2012), Large volcanic aerosol load in the stratosphere linked to Asian monsoon transport, *Science*, *337*(6090), 78–81.

CCMVal, S. (2010), SPARC report on the evaluation of chemistry-climate models, SPARC report, (5).

Chen, P. (1995), Isentropic cross-tropopause mass exchange in the extratropics, *J. Geophys. Res.*, *100*(D8), 16,661–16,673.

Forster, P. M., and K. P. Shine (1999), Stratospheric water vapor changes as a possible contributor to observed stratospheric cooling, *Geophys. Res. Lett.*, *26*, 3309–3312.

Douglass, A., R. Stolarski, M. Schoeberl, C. Jackman, M. Gupta, P. Newman, J. Nielsen, and E. Fleming (2008), Relationship of loss, mean age of air and the distribution of CFCs to stratospheric circulation and implications for atmospheric lifetimes, *J. Geophys. Res.*, *113*, D14309, doi:10.1029/2007JD009575.

Douglass, A. R., C. J. Weaver, R. B. Rood, and L. Coy (1996), A three-dimensional simulation of the ozone annual cycle using winds from a data assimilation system, *J. Geophys. Res.*, *101*(D1), 1463–1474.

Forster, P. M. d. F., and K. Shine (2002), Assessing the climate impact of trends in stratospheric water vapor, *Geophys. Res. Lett.*, *29*(6), 1086, doi:10.1029/2001GL013909.

Fueglistaler, S., H. Wernli, and T. Peter (2004), Tropical troposphere-to-stratosphere transport inferred from trajectory calculations, *J. Geophys. Res.*, *109*, D03108, doi:10.1029/2003JD004069.

Gettelman, A., D. E. Kinnison, T. J. Dunkerton, and G. P. Brasseur (2004), Impact of monsoon circulations on the upper troposphere and lower stratosphere, *J. Geophys. Res.*, *109*, D22101, doi:10.1029/2004JD004878.

Haine, T., H. Zhang, D. Waugh, and M. Holzer (2008), On transit-time distributions in unsteady circulation models, *Ocean Modell.*, *21*(1), 35–45.

Haine, T. W., and T. M. Hall (2002), A generalized transport theory: Water-mass composition and age, *J. Phys. Oceanogr.*, *32*(6), 1932–1946.

Hall, T. M., and R. A. Plumb (1994), Age as a diagnostic of stratospheric transport, *J. Geophys. Res.*, *99*(D1), 1059–1070.

Hofmann, D., J. Barnes, M. O'Neill, M. Trudeau, and R. Neely (2009), Increase in background stratospheric aerosol observed with lidar at Mauna Loa Observatory and Boulder, Colorado, *Geophys. Res. Lett.*, *36*, L15808, doi:10.1029/2009GL039008.

Holzer, M., and T. M. Hall (2000), Transit-time and tracer-age distributions in geophysical flows, *J. Atmos. Sci.*, *57*(21), 3539–3558.

Holzer, M., F. W. Primeau, W. M. Smethie, and S. Khatiwala (2010), Where and how long ago was water in the western North Atlantic ventilated? Maximum entropy inversions of bottle data from WOCE line A20, *J. Geophys. Res.*, *115*, C07005, doi:10.1029/2009JC005750.

Hossaini, R., M. Chipperfield, S. Montzka, A. Rap, S. Dhomse, and W. Feng (2015), Efficiency of short-lived halogens at influencing climate through depletion of stratospheric ozone, *Nat. Geosci.*, *8*, 186–190.

Khatiwala, S., F. Primeau, and T. Hall (2009), Reconstruction of the history of anthropogenic CO_2 concentrations in the ocean, *Nature*, *462*(7271), 346–349.

Khatiwala, S., F. Primeau, and M. Holzer (2012), Ventilation of the deep ocean constrained with tracer observations and implications for radiocarbon estimates of ideal mean age, *Earth Planet. Sci. Lett.*, *325*, 116–125.

Konopka, P., J.-U. Grooß, F. Plöger, and R. Müller (2009), Annual cycle of horizontal in-mixing into the lower tropical stratosphere, *J. Geophys. Res.*, *114*, D19111, doi:10.1029/2009JD011955.

Liang, Q., R. Stolarski, S. Kawa, J. Nielsen, A. Douglass, J. Rodriguez, D. Blake, E. Atlas, and L. Ott (2010), Finding the missing stratospheric Br_y: A global modeling study of $CHBr_3$ and CH_2Br_2, *Atmos. Chem. Phys.*, *10*(5), 2269–2286.

Lin, S.-J., and R. B. Rood (1996), Multi-dimensional flux-form semi-Lagrangian transport schemes, *Mon. Weather Rev.*, *124*(9), 2046–2070.

Lu, J., G. A. Vecchi, and T. Reichler (2007), Expansion of the Hadley cell under global warming, *Geophys. Res. Lett.*, *34*, L06805, doi:10.1029/2006GL028443.

McCarthy, J. J. (2001), *Climate Change 2001: Impacts, Adaptation, and Vulnerability: Contribution of Working Group II to the Third Assessment Report of the Intergovernmental Panel on Climate Change*, Cambridge Univ. Press, Cambridge, U. K.

Molod, A., L. Takacs, M. Suarez, J. Bacmeister, I.-S. Song, and A. Eichmann (2012), The GEOS-5 atmospheric general circulation model: Mean climate and development from MERRA to Fortuna, NASA Technical Report Series on Global Modeling and Data Assimilation, NASA TM—2012-104606, vol. 28, 117 pp.

Moorthi, S., and M. J. Suarez (1992), Relaxed Arakawa-Schubert. A parameterization of moist convection for general circulation models, *Mon. Weather Rev.*, *120*(6), 978–1002.

Neely, R., et al. (2013), Recent anthropogenic increases in SO_2 from Asia have minimal impact on stratospheric aerosol, *Geophys. Res. Lett.*, *40*, 999–1004, doi:10.1002/grl.50263.

Neu, J. L., and R. A. Plumb (1999), Age of air in a leaky pipe model of stratospheric transport, *J. Geophys. Res.*, *104*(D16), 19,243–19,255.

Orbe, C., M. Holzer, L. M. Polvani, and D. Waugh (2013), Air-mass origin as a diagnostic of tropospheric transport, *J. Geophys. Res. Atmos.*, *118*, 1459–1470, doi:10.1002/jgrd.50133.

Orbe, C., P. A. Newman, D. W. Waugh, M. Holzer, L. D. Oman, F. Li, and L. M. Polvani (2015), Air-mass origin in the Arctic. Part I: Seasonality, *J. Clim.*, doi:10.1175/JCLI-D-14-00720.1, in press.

Ott, L., S. Pawson, and J. Bacmeister (2011), An analysis of the impact of convective parameter sensitivity on simulated global atmospheric CO distributions, *J. Geophys. Res.*, *116*, D21310, doi:10.1029/2011JD016077.

Park, M., W. J. Randel, D. E. Kinnison, R. R. Garcia, and W. Choi (2004), Seasonal variation of methane, water vapor, and nitrogen oxides near the tropopause: Satellite observations and model simulations, *J. Geophys. Res.*, *109*, D03302, doi:10.1029/2003JD003706.

Park, M., W. J. Randel, D. E. Kinnison, L. K. Emmons, P. F. Bernath, K. A. Walker, C. D. Boone, and N. J. Livesey (2013), Hydrocarbons in the upper troposphere and lower stratosphere observed from ACE-FTS and comparisons with WACCM, *J. Geophys. Res. Atmos.*, *118*, 1964–1980, doi:10.1029/2012JD018327.

Pawson, S., R. S. Stolarski, A. R. Douglass, P. A. Newman, J. E. Nielsen, S. M. Frith, and M. L. Gupta (2008), Goddard Earth Observing System Chemistry-Climate Model simulations of stratospheric ozone-temperature coupling between 1950 and 2005, *J. Geophys. Res.*, *113*, D12103, doi:10.1029/2007JD009511.

Ploeger, F., G. Günther, P. Konopka, S. Fueglistaler, R. Müller, C. Hoppe, A. Kunz, R. Spang, J.-U. Grooß, and M. Riese (2013), Horizontal water vapor transport in the lower stratosphere from subtropics to high latitudes during boreal summer, *J. Geophys. Res. Atmos.*, *118*, 8111–8127, doi:10.1002/jgrd.50636.

Plumb, R. A. (1996), A tropical pipe model of stratospheric transport, *J. Geophys. Res.*, *101*(D2), 3957–3972.

Randel, W. J., M. Park, L. Emmons, D. Kinnison, P. Bernath, K. A. Walker, C. Boone, and H. Pumphrey (2010), Asian monsoon transport of pollution to the stratosphere, *Science*, *328*(5978), 611–613.

Randel, W. J., E. Moyer, M. Park, E. Jensen, P. Bernath, K. Walker, and C. Boone (2012), Global variations of HDO and HDO/H_2O ratios in the upper troposphere and lower stratosphere derived from ACE-FTS satellite measurements, *J. Geophys. Res.*, *117*, D06303, doi:10.1029/2011JD016632.

Rosenlof, K. H., A. F. Tuck, K. K. Kelly, J. M. Russell, and M. P. McCormick (1997), Hemispheric asymmetries in water vapor and inferences about transport in the lower stratosphere, *J. Geophys. Res.*, *102*(D11), 13,213–13,234.

Shindell, D. T. (2001), Climate and ozone response to increased stratospheric water vapor, *Geophys. Res. Lett.*, *28*(8), 1551–1554.

Sinnhuber, B.-M., et al. (2002), Comparison of measurements and model calculations of stratospheric bromine monoxide, *J. Geophys. Res.*, *107*(D19), 4398, doi:10.1029/2001JD000940.

Solomon, S., J. S. Daniel, R. Neely, J.-P. Vernier, E. G. Dutton, and L. W. Thomason (2011), The persistently variable background stratospheric aerosol layer and global climate change, *Science*, *333*(6044), 866–870.

Stolarski, R. S., D. W. Waugh, L. Wang, L. D. Oman, A. R. Douglass, and P. A. Newman (2014), Seasonal variation of ozone in the tropical lower stratosphere: Southern tropics are different from northern tropics, *J. Geophys. Res. Atmos.*, *119*, 6196–6206, doi:10.1002/2013JD021294.

Suarez, M. J., et al. (2008), The GEOS-5 Data Assimilation System—Documentation of Versions 5.0.1, 5.1.0, and 5.2.0.

Thomason, L., and J.-P. Vernier (2013), Improved SAGE II cloud/aerosol categorization and observations of the Asian tropopause aerosol layer: 1989–2005, *Atmos. Chem. Phys.*, *13*(9), 4605–4616.

Tomczak, M. (1981), A multi-parameter extension of temperature/salinity diagram techniques for the analysis of non-isopycnal mixing, *Prog. Oceanogr.*, *10*(3), 147–171.

Vernier, J.-P., L. Thomason, and J. Kar (2011a), CALIPSO detection of an Asian tropopause aerosol layer, *Geophys. Res. Lett.*, *38*, L07804, doi:10.1029/2010GL046614.

Vernier, J.-P., et al. (2011b), Major influence of tropical volcanic eruptions on the stratospheric aerosol layer during the last decade, *Geophys. Res. Lett.*, *38*, L12807, doi:10.1029/2011GL047563.

Vogel, B., G. Günther, R. Müller, J.-U. Grooß, P. Hoor, M. Krämer, S. Müller, A. Zahn, and M. Riese (2014), Fast transport from Southeast Asia boundary layer sources to northern Europe: Rapid uplift in typhoons and eastward eddy shedding of the Asian monsoon anticyclone, *Atmos. Chem. Phys.*, *14*(23), 12,745–12,762.

WMO (2007), Scientific assessment of ozone depletion: 2006, *World Meteorological Organisation, Global Ozone Research and Monitoring Project-Report, 50, 572*.